

PERFORMANCE ENHANCEMENT OF A THREE DIMENSIONAL OCDMA SYSTEMS BASED ON A NEW CODE

^{1,5}RASIM AZEEZ KADHIM, ²HILAL ADNAN FADHIL, ³S.A. ALJUNID, ⁴MOHAMAD SHAHRAZEL RAZALLI,

^{1,2,3,4}School of Computer and Communication Engineering, Universiti Malaysia Perlis (UniMAP), Pauh Putra, Arau, Perlis 02600, Malaysia

⁵Ministry of Sciences and Technology, Baghdad, Iraq

E-mail: ¹rasmaziz@yahoo.com, ²hilaladnan@unimap.edu.my, ³syedalwee@unimap.edu.my, ⁴mohamad@unimap.edu.my.

ABSTRACT

In this paper, we propose a three dimensional (3-D) codes namely 3-D perfect difference/ multi diagonal (3-D PD/MD) code for spectral/time/spatial optical code division multiple access (OCDMA) system based on the perfect difference and multi diagonal codes. The multi-access interference (MAI) is fully eliminated in the receiver based on this code. The system performance is analyzed mathematically based on the proposed code under the consideration of the receiver noises, and compared with the systems of , 2-D perfect difference (2-D PD), 2-D diluted perfect difference (2-D DPD) and 3-D perfect difference (3-D PD) code. The proposed code reduces the receiver noises by reducing the receiver complexity to 50% of the 3-D PD code. In addition to that, the mathematical results shows that the 3-D PD/MD code system can accommodate more active users at a bit error rate (BER) of (10^{-9}) and data rates of 0.622Gbps and 1.25Gbps. Hence, the proposed system can be more applicable than the former 3-D PD code.

Keywords: *Optical Code Division Multiple Access (OCDMA), Perfect Difference (PD) Codes, Phase-Induced Intensity Noise (PIIN).*

1. INTRODUCTION

The concept of optical code division multiple access (OCDMA) technique was borrowed from the wireless CDMA during the 8th decade of the 20th century, in which each user is assigned by a unique address code in the network. The code is a sequence of ones and zeros that can be designed by a mathematical formula or algorithm. The system performance was affected by the interference from the other active users which is called multiple-access interference (MAI), and the receiver noises represented by the phase-induced intensity noise (PIIN), shot noise and thermal noise. Initially, the one dimensional (1-D) codes were proposed by spreading the optical pulses in one dimension. Many codes have been presented for incoherent OCDMA systems based on the time spreading [1]–[3]. Moreover, another codes exploited the frequency (wavelength) domain and constructed the spectral amplitude coding optical code division multiple access (SAC-OCDMA) systems [4]–[9]. A drawback of 1-D codes is the increase in code length as the number of simultaneous users increases.

The second approach exploiting two dimensions (2-D) by combining of (time/spectral, spectral/spatial, time/spatial) codes have been proposed with shorter code length than the 1-D to enhance the system performance by mitigating the receiver noises and increasing the number of active users [10]–[13]. The third approach uses three dimensions (3-D) to decrease the code length and further increasing the number of users. Yeh *et al.* [14], proposed the 3-D perfect difference (3-D PD) codes with the structure of a spectral/time/spatial OCDMA system. The authors proved that the 3-D PD code can achieve more number of active users compared to those of previous codes with the same total code size.

In this paper, a new 3-D perfect difference/multi diagonal (3-D PD/MD) code is proposed to reduce the receiver complexity and enhance the performance of the 3D-PD code. The BER expression of the OCDMA systems based on the proposed code is presented undertaken the effects of PIIN, shot noise, and thermal noise. The comparison results of the proposed code with that of the related codes, such as the 2-D perfect difference (2-D PD), 2-D diluted perfect difference (2-D DPD) and 3D-PD codes revealed that the



proposed system provides better performance than the other systems.

2. 3-D PERFECT DIFFERENCE/MULTI DIAGONAL CODE CONSTRUCTION

The construction of the 3-D PD/MD codes depends on the PD code [3], and MD code [9]. These two codes are constructed as follows in subsections (2.1, 2.2) :

2.1 The Multi Diagonal (MD) Code

In 2011, Abd et. al. proposed a new code for incoherent SAC-OCDMA namely Multi Diagonal (MD) code to enhance the SAC-OCDMA system performance with lower complexity. The MD code has the zero cross correlation property where it constructed without overlap between any codeword, not restricted for the number of users and the value of the weight, therefore a good system performance was achieved in terms of BER, number of active users and transmission data rate. The basic idea of this code based on the orthogonality between the elements of identity matrix. An example of MD code for w=2 and the number of users is 6, is presented in Table 1.

Table 1: 1-D MD Codes For w = 2

i	MD Codes
0	100000000001
1	010000000010
2	001000000100
3	000100001000
4	000010010000
5	000001100000

2.2 The Perfect Difference (PD) Code

The generation of the PD codes of (N, w, λ) from the perfect difference sets was explained in [3]. The weight, length, and size of the code are w, N, and N respectively, where N = w² - w + 1. Table 2 shows an example of the PD

codes for w = 3. The expression of the correlation θ_{xy} between different codes C_x and C_y is:

$$\theta_{xy} = \begin{cases} w & x = y \\ 1 & x \neq y \end{cases} \quad (1)$$

Table 2: The PD Codes For w = 3

i	Cyclic Difference Sets	PD Codes
0	{ 0 1 3 }	1101000
1	{ 0 2 6 }	1010001
2	{ 1 5 6 }	0100011
3	{ 0 4 5 }	1000110
4	{ 3 4 6 }	0001101
5	{ 2 3 5 }	0011010
6	{ 1 2 4 }	0110100

2.3 The 3-D PD/MD Code

The 3-D PD/MD code can be constructed by combining two PD codes for spectral and time domains, and MD code for spatial domain. Let the PD codes are X = {x₀, x₁, ..., x_{M-1}} and Y = {y₀, y₁, ..., y_{N-1}} with the code lengths and sizes, M = w₁² - w₁ + 1, N = w₂² - w₂ + 1 where, w₁ and w₂ are the code weights of X, and Y, respectively; and the MD code is Z = {z₀, z₁, ..., z_{P-1}} with a code length of P = P_s * w₃ where w₃ and P_s are the weight and the size of the code, respectively. The groups of codes for each domain are X_e, Y_f, and Z_l where e = 0, 1, ..., M - 1, f = 0, 1, ..., N - 1, and l = 0, 1, ..., P_s - 1. The system cardinality will be equal to the multiplication of these three code sizes MNP_s.

The expression of the 3-D PD/MD code is B_{e,f,l} = X_e^TY_fZ_l, where Z_l is a matrix of Z elements multiplied by the unity matrix of N × N dimension. Then, B_{e,f,l} can be expressed as in equ. (2).

$$B_{e,f,l} = \begin{bmatrix} b_{0,0,0} & b_{0,1,0} & \dots & b_{0,N-1,0} & b_{0,0,1} & b_{0,1,1} & \dots & b_{0,N-1,1} & b_{0,0,P-1} & b_{0,1,P-1} & \dots & b_{0,N-1,P-1} \\ b_{1,0,0} & b_{1,1,0} & \dots & b_{1,N-1,0} & b_{1,0,1} & b_{1,1,1} & \dots & b_{1,N-1,1} & b_{1,0,P-1} & b_{1,1,P-1} & \dots & b_{1,N-1,P-1} \\ \vdots & \vdots & \vdots & \vdots & \vdots & \vdots & \vdots & \vdots & \vdots & \vdots & \vdots & \vdots \\ b_{M-1,0,0} & b_{M-1,1,0} & \dots & b_{M-1,N-1,0} & b_{M-1,0,1} & b_{M-1,1,1} & \dots & b_{M-1,N-1,1} & b_{M-1,0,P-1} & b_{M-1,1,P-1} & \dots & b_{M-1,N-1,P-1} \end{bmatrix} \quad (2)$$



To explain the cross correlation of the 3-D PD/MD codes, an eight characteristic matrices $B^a, a \in (0,1, \dots, 7)$ can be introduced as below:

$$\begin{aligned}
 B_{e,f,l}^{(0)} &= X_e^T Y_f Z_l & B_{e,f,l}^{(1)} &= X_e^T \bar{Y}_f Z_l \\
 B_{e,f,l}^{(2)} &= \bar{X}_e^T Y_f Z_l & B_{e,f,l}^{(3)} &= \bar{X}_e^T \bar{Y}_f Z_l \\
 B_{e,f,l}^{(4)} &= X_e^T Y_f \bar{Z}_l & B_{e,f,l}^{(5)} &= X_e^T \bar{Y}_f \bar{Z}_l \\
 B_{e,f,l}^{(6)} &= \bar{X}_e^T Y_f \bar{Z}_l & B_{e,f,l}^{(7)} &= \bar{X}_e^T \bar{Y}_f \bar{Z}_l
 \end{aligned} \tag{3}$$

Where \bar{X} and \bar{Y} are the complementary of X and Y , respectively. \bar{Z} is the complementary of Z sequence multiplied each element by the identity matrix with dimension $N \times N$. So that, the cross correlation

between the characteristic matrix $B_{e,f,l}^{(a)}$ and any code matrix $B_{e,f,l}$ is defined as follows. The cross correlation properties of the 3-D PD/MD codes are presented in Table 3 .

$$R^{(a)}(e, f, l) = \sum_{i=0}^{M-1} \sum_{j=0}^{N-1} \sum_{h=0}^{P-1} b_{i,j,h}^{(a)} \cdot b_{i,j,h} \tag{4}$$

Table 3 can be divided into two independent groups, the upper part includes $(R^{(0)}(e, f, l), R^{(1)}(e, f, l), R^{(2)}(e, f, l), R^{(3)}(e, f, l))$ and the lower part includes $(R^{(4)}(e, f, l), R^{(5)}(e, f, l), R^{(6)}(e, f, l), R^{(7)}(e, f, l))$. However, the groups are the same, hence any one can be used to construct the receiver. The receiver equation to eliminate the MAI according to the upper group is :

$$\begin{aligned}
 &R^{(0)}(e, f, l) - \frac{R^{(1)}(e, f, l)}{(w_2 - 1)} - \frac{1}{(w_1 - 1)} \left[R^{(2)}(e, f, l) - \frac{R^{(3)}(e, f, l)}{(w_2 - 1)} \right] \\
 &= \begin{cases} w_1 w_2 w_3 & e = 0, f = 0, l = 0 \\ 0 & otherwise \end{cases} \tag{5}
 \end{aligned}$$

Table 3: The Cross Correlation Properties Of The 3-D PD/MD Code

	$R^{(0)}(e,f,l)$	$R^{(1)}(e,f,l)$	$R^{(2)}(e,f,l)$	$R^{(3)}(e,f,l)$
$e=0 \cap f=0 \cap l=0$	$w_1 w_2 w_3$	0	0	0
$e \neq 0 \cap f=0 \cap l=0$	$w_2 w_3$	0	$w_2 w_3 (w_1 - 1)$	0
$e=0 \cap f \neq 0 \cap l=0$	$w_1 w_3$	$w_1 w_3 (w_2 - 1)$	0	0
$e \neq 0 \cap f \neq 0 \cap l=0$	w_3	$w_3 (w_2 - 1)$	$w_3 (w_1 - 1)$	$w_3 (w_2 - 1) (w_1 - 1)$
$e=0 \cap f=0 \cap l \neq 0$	0	0	0	0
$e \neq 0 \cap f=0 \cap l \neq 0$	0	0	0	0
$e=0 \cap f \neq 0 \cap l \neq 0$	0	0	0	0
$e \neq 0 \cap f \neq 0 \cap l \neq 0$	0	0	0	0

	$R^{(4)}(e,f,l)$	$R^{(5)}(e,f,l)$	$R^{(6)}(e,f,l)$	$R^{(7)}(e,f,l)$
$e=0 \cap f=0 \cap l=0$	0	0	0	0
$e \neq 0 \cap f=0 \cap l=0$	0	0	0	0
$e=0 \cap f \neq 0 \cap l=0$	0	0	0	0
$e \neq 0 \cap f \neq 0 \cap l=0$	0	0	0	0
$e=0 \cap f=0 \cap l \neq 0$	$w_1 w_2 w_3$	0	0	0
$e \neq 0 \cap f=0 \cap l \neq 0$	$w_2 w_3$	0	$w_2 w_3 (w_1 - 1)$	0
$e=0 \cap f \neq 0 \cap l \neq 0$	$w_1 w_3$	$w_1 w_3 (w_2 - 1)$	0	0
$e \neq 0 \cap f \neq 0 \cap l \neq 0$	w_3	$w_3 (w_2 - 1)$	$w_3 (w_1 - 1)$	$w_3 (w_2 - 1) (w_1 - 1)$

3. TRANSMITTER/RECEIVER DESCRIPTION

The transmitter of OCDMA system based on the proposed code is shown in Figure 1. The operation of the transmitter is as follows: the optical pulses from the incoherent light source are modulated according to the ON-OFF keying format of the data bits through an electrical to optical modulator (EOM). Then, three stages are used to encode these pulses in three dimensions; the first stage applies in spectral domain by using the Fiber Brag Grating (FBG) in which the spectral components with wavelengths matched to '1' of the spectral code sequence X_e are reflected back by FBGt1 and the other wavelengths are filtered out, the reflected spectral components are passed through the FBGt2 to reflect it again for compensating the run-trip delay because the FBGt2 has an opposite arrangement of FBGt1. The second stage encodes the reflected spectral components of optical pulses in time domain by using the optical delay lines. The output of the second stage is split into w_2 equal parts and pass through w_2 optical delay lines with different time delays according to the code sequence Y_f , then it is combined in the other side. The third stage represents the encoding in spatial domain where the arrival optical pulses are split into w_3 equal parts in order to transmit it to the star coupler according to the spatial code sequence of Z_l .

The structure of the receiver according to equ. (5) is shown in Figure 2, in which it includes a combiner, two correlators, two balanced detectors and an integrator. The opposite sequence is adopted to decode the optical signal in the receiver side. The combiner is used to aggregate the incoming optical signals from the star couplers according to the code sequence Z_l . Then, the correlators are used to disperse the signals in time domain. The correlator 1 and correlator 2 consist of w_2 and $N - w_2$ optical delay lines of different delays based on the code sequence Y_f and \bar{Y}_f respectively. After that, two balanced detectors are used to decode the signal in spectral domain. The decoding process is similar to the encoding process in the transmitter where the FBGr2 and FBGr4 are used to reflect back the same spectral components which are matched to "1s" of the spectral code sequence X_e , while the FBGr1 and FBGr3 are used to compensate the run-trip delays. Finally the aggregated signal from all photodetectors is integrated by the integrator over the chip period.

According to the equ. (5), the output currents of PDs(0,1,2,3) are respectively proportional to $R^{(0)}(e, f, l)$, $R^{(1)}(e, f, l)/(w_2 - 1)$, $R^{(2)}(e, f, l)/(w_1 - 1)$, $R^{(3)}(e, f, l)/(w_2 - 1)(w_1 - 1)$.

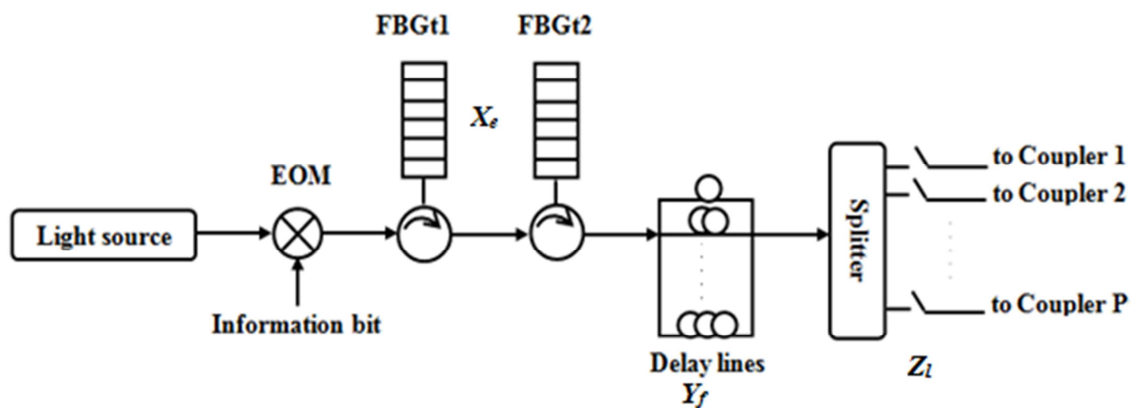


Figure 1. The 3-D PD/MD Code Transmitter Structure.

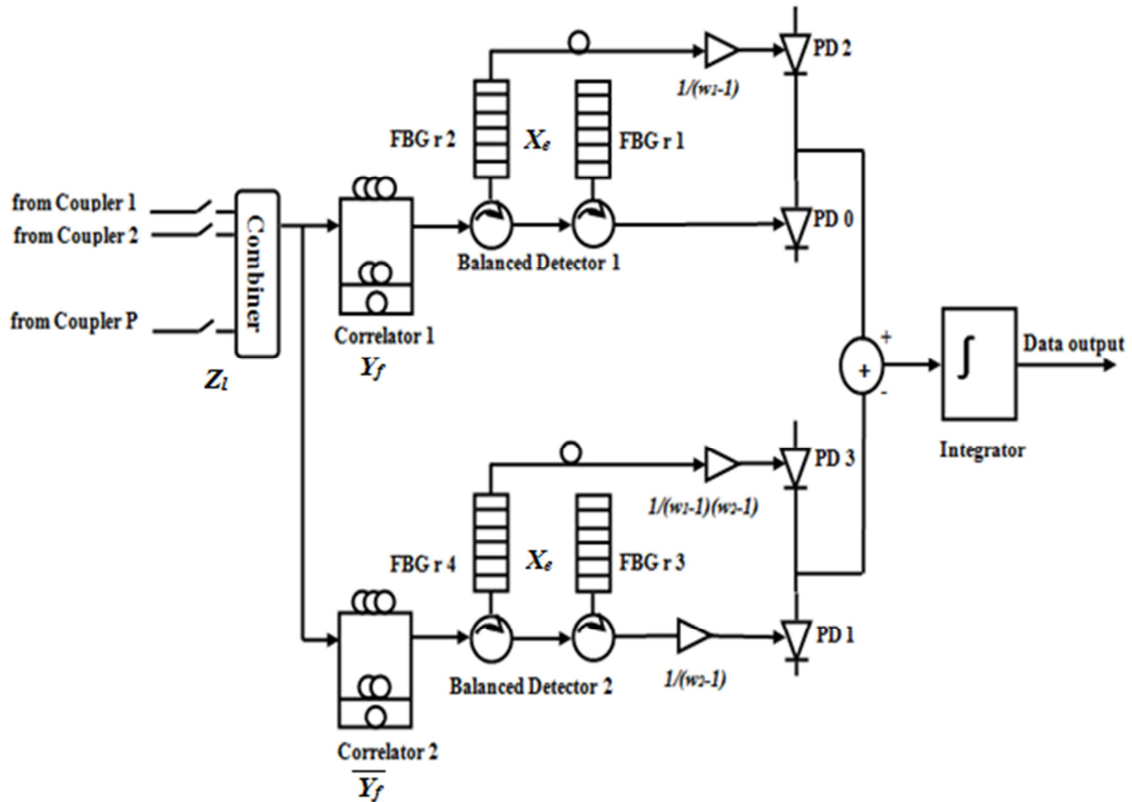


Figure. 2. The 3-D PD/MD Code Receiver Structure.

4. SYSTEM PERFORMANCE

This section presents the derivation of a mathematical expression of the signal to noise ratio (SNR) and the bit error rate (BER) under the consideration of the receiver noises represented by the shot, PIIN and thermal noise. The BER is estimated based on Gaussian approximation. The SNR is the ratio between the square of the average current and the total noise currents as follows [6]

$$SNR = \frac{I_r^2}{\langle i^2_{noise} \rangle} \tag{6}$$

Where I_r is the average photodetector current, and $\langle i^2_{noise} \rangle$ is the variance of the receiver noises current which can be expressed by:

$$\begin{aligned} \langle i^2_{noise} \rangle &= \langle i^2_{PIIN} \rangle + \langle i^2_{shot} \rangle + \langle i^2_{thermal} \rangle \\ &= B_w I_r^2 \tau_r + 2eB_w I_{total} + \frac{4K_b T_n B_w}{R_L} \end{aligned} \tag{7}$$

Where B_w is the electrical bandwidth, e is the electron charge, R_L is the load resistance, K_b is Boltzman's constant, I_{total} is the total photocurrent, and τ_r is the coherence time of the light which expressed as [6]:

$$\tau_r = \frac{\int_0^\infty S^2(v) dv}{[\int_0^\infty S(v) dv]^2} \tag{8}$$

Where $S(v)$ is the single sideband power spectral density.

The analysis is simplified based on four assumptions [5]: a) The broadband light source is ideally unpolarized and its spectrum is flat over $[v_0 - \Delta v/2, v_0 + \Delta v/2]$ and emits equal power, where v_0 is the central optical frequency and Δv is the optical source bandwidth. b) Each spectral component produced by the spectral encoders has identical spectral width. c) Each spectral component received by a user has the same power. d) Each bit stream from each user is synchronized. We defined $F(v, i)$ as follows:

$$F(v, i) = \left\{ u \left[v - v_0 - \frac{\Delta v}{2M} (-M + 2i) \right] - u \left[v - v_0 - \frac{\Delta v}{2M} (-M + 2i + 2) \right] \right\} \quad I_1 = \mathcal{R} \int_0^\infty G_1(v) dv \quad (9)$$

Where $u(v)$ is a unit step function defined as:

$$u(v) = \begin{cases} 1 & v \geq 0 \\ 0 & v < 0 \end{cases} \quad (10)$$

Based on the assumptions above, the PSD of the received signals can be written as:

$$r(v) = \frac{P_{sr}}{w_2 w_3 \Delta v} \times \sum_{k=1}^K d(k) \sum_{h=0}^{P-1} \sum_{i=0}^{M-1} \sum_{j=0}^{N-1} b_{(i,j,h)}(k) F(v, i) \quad (11)$$

$$= \frac{\mathcal{R} P_{sr}}{w_2 w_3 M} \left\{ \frac{w_3 w_1 (K-1)(N-1)}{(MNP_s - 1)} + \frac{w_3 (K-1)(N-1)(M-1)}{(MNP_s - 1)} \right\} \quad (13)$$

Where P_{sr} is the effective source power at the receiver, K is the number of active users, $d(k)$ is the data bit of k th user which can be '1' or '0', M , N and P are the code lengths of spectral, time spreading and spatial code sequences respectively, and $b_{i,j,h}(k)$ is an element of the k th user's codeword.

Since all receivers have the same structure and property, the derivation will be done on receiver $(0,0,0)$. The output currents of PDs $(0,1,2,3)$ can be obtained depending on the cross correlation between $B_{0,0,0}^{(a)}$ and $B_{e,f,l}$ as follows:

$$I_0 = \mathcal{R} \int_0^\infty G_0(v) dv$$

$$= \int_0^\infty \frac{\mathcal{R} P_{sr}}{w_2 w_3 \Delta v} \times \sum_{k=1}^K d(k) R^{(0)}(i, j, h) F(v, i) dv$$

$$= \frac{\mathcal{R} P_{sr}}{w_2 w_3 M} \left\{ w_3 w_1 w_2 + \frac{w_2 w_3 (K-1)(M-1)}{(MNP_s - 1)} + \frac{w_3 w_1 (K-1)(N-1)}{(MNP_s - 1)} + \frac{w_3 (K-1)(N-1)(M-1)}{(MNP_s - 1)} \right\} \quad (12)$$

$$I_2 = \mathcal{R} \int_0^\infty G_2(v) dv$$

$$= \int_0^\infty \frac{\mathcal{R} P_{sr}}{(w_1 - 1) w_2 w_3 \Delta v} \times \sum_{k=1}^K d(k) R^{(2)}(i, j, h) F(v, i) dv$$

$$= \frac{\mathcal{R} P_{sr}}{w_2 w_3 M} \left\{ \frac{w_2 w_3 (K-1)(M-1)}{(MNP_s - 1)} + \frac{w_3 (K-1)(N-1)(M-1)}{(MNP_s - 1)} \right\} \quad (14)$$

$$I_3 = \mathcal{R} \int_0^\infty G_3(v) dv$$

$$= \int_0^\infty \frac{\mathcal{R} P_{sr}}{(w_2 - 1)(w_1 - 1) w_2 w_3 \Delta v} \times \sum_{k=1}^K d(k) R^{(3)}(i, j, h) F(v, i) dv$$

$$= \frac{\mathcal{R} P_{sr}}{w_2 w_3 M} \left\{ \frac{w_3 (K-1)(N-1)(M-1)}{(MNP_s - 1)} \right\} \quad (15)$$

Where \mathcal{R} is the responsivity of the photodiode.

The average output photocurrent is :-

$$I_r = \mathcal{R} \int_0^\infty \{ [G_0(v) - G_2(v)] - [G_1(v) - G_3(v)] \} dv$$

$$= [I_0 - I_1 - I_2 + I_3]$$

$$= \frac{\mathcal{R}P_{sr}w_1}{M} \quad (16)$$

The PIIN current is presented as follows:

$$\langle i^2_{PIIN} \rangle = B_w \mathcal{R}^2 I_r^2 \tau_r$$

$$= B_w \mathcal{R}^2 I_r^2 \frac{\int_0^\infty [G_0(v) - G_1(v) - G_2(v) + G_3(v)]^2 dv}{\left\{ \int_0^\infty [G_0(v) - G_1(v) - G_2(v) + G_3(v)] dv \right\}^2}$$

$$= B_w \mathcal{R}^2 \int_0^\infty [G_0(v) - G_1(v) - G_2(v) + G_3(v)]^2 dv \quad (17)$$

Since $G_0(v)$ and $G_1(v)$ do not overlap with $G_2(v)$ and $G_3(v)$, so that $\langle i^2_{PIIN} \rangle$ is:

$$\langle i^2_{PIIN} \rangle = B_w \mathcal{R}^2 \int_0^\infty [G_0^2(v) + G_1^2(v) + G_2^2(v) + G_3^2(v) - 2G_0(v)G_1(v) - 2G_2(v)G_3(v)] dv \quad (18)$$

The integral of each part can be obtained separately and then combined together under the worst scenario when all users send bit '1' to get:

$$\langle i^2_{PIIN} \rangle = \frac{MB_w}{\Delta v} \left\{ \frac{(I_0 - I_1)^2}{w_1} + \frac{(I_2 - I_3)^2}{(w_1 - 1)^2} \right\} \quad (19)$$

Because of the probability of sending bit '1' or '0' is 0.5 for each user, the $\langle i^2_{PIIN} \rangle$ will be:

$$\langle i^2_{PIIN} \rangle = \frac{MB_w}{2\Delta v} \left\{ \frac{(I_0 - I_1)^2}{w_1} + \frac{(I_2 - I_3)^2}{(w_1 - 1)^2} \right\} \quad (20)$$

Then $\langle i^2_{shot} \rangle$ with 0.5 probability of sending '1' or '0' can be expressed:

$$\langle i^2_{shot} \rangle = 2eB_w I_{total} / 2$$

$$= eB_w (I_0 + I_1 + I_2 + I_3) \quad (21)$$

The effect of thermal noise can be expressed as:

$$\langle i^2_{thermal} \rangle = \frac{4K_b T_n B_w}{R_L} \quad (22)$$

The average signal to noise ratio SNR can be calculated by substitute equ. (16), (20), (21) and (22) in equ. (6) :

$$SNR = \frac{\left(\frac{\mathcal{R}P_{sr}w_1}{M} \right)^2}{\frac{MB_w}{2\Delta v} \left\{ \frac{(I_0 - I_1)^2}{w_1} + \frac{(I_2 - I_3)^2}{(w_1 - 1)^2} \right\} + eB_w (I_0 + I_1 + I_2 + I_3) + \frac{4K_b T_n B_w}{R_L}}$$

$$(23)$$

And the BER is [6]:

$$BER = \frac{\text{erfc} \left(\sqrt{\frac{SNR}{8}} \right)}{2}, \quad (24)$$

Where

$$\text{erfc}(z) = \frac{2}{\sqrt{\pi}} \int_z^\infty \exp(-y^2) dy. \quad (25)$$

5. NUMERICAL RESULTS

The performance of the 3-D PD/MD code with ($M = 7, N = 13, Ps = 3$) and the previously presented 2-D PD and 3-D PD codes in the presence of the PIIN, the photodiode shot noise, and the thermal noise are illustrated in Fig.3 and Fig.4 for a data rate of 0.622Gbps and 1.25Gbps respectively. The system parameters used in the numerical analysis are: Spectral width of light $\Delta v = 5\text{THz}$, Broadband effective power $P_{sr} = -10\text{dBm}$, Operating wavelength $\lambda_0 = 1550\text{nm}$, receiver noise temperature $T_n = 300\text{Kelvin}$, responsivity of photo detector $R = 0.75$, receiver load resistance $R_L = 1030\ \Omega$. The receiver electrical bandwidth B_w was chosen as 0.5 of the data rate for the 2-D PD and 2-D DPD codes, and $0.5 * N$ of the data rate for the 3-D PD and 3-D PD/MD codes.

Figure 3 shows the number of active users versus the BER for the proposed code and the codes under comparison with the data bit rate of 0.622Gbps. The performance of the 3-D PD/MD code is better than the others. At BER of (10^{-9}) the 3-D PD/MD code can accommodate 180 users in comparison to 165, 135 and 112 users for the 3-D PD, 2-D DPD

and 2-D PD codes ,respectively. Moreover, Figure 4 shows the same relation with the data bit rate of 1.25Gbps. The figure demonstrates that the system performance with the 3-D PD/MD code is still better than the other codes by accommodating more active users in spite of the increasing the data rate. However, the increasing of number of active users of the 3-D PD/MD code over the 3-D PD code is limited, but the proposed system reduces the complexity of the receiver by 50% to be more applicable than the former one.

The relation between the BER and the effective received power in dBm at a data bit rate equal to 0.622Gbps and the number of active users is 150 for different codes can be shown in Figure 5. It is obvious that the proposed code has a minimum

BER in the range of -25dBm to -5dBm but the performance of 3-D PD/MD and 3-D PD are very closed at high power. That is because the proposed code has the ability to reduce the effect of the shot noise by reducing the number of photodetectors while it has the same ability of the 3-D PD code in mitigation of the PIIN.

The data rate of each user versus the BER for 150 active users and $P_{sr} = -10\text{dBm}$, is shown in Figure 6. At BER of 10^{-9} , the proposed code achieves the highest data rate of 0.8Gbps in comparison to 0.7, 0.55 and 0.4Gbps for the 3-D PD, 2-D DPD and 2-D PD codes, respectively.

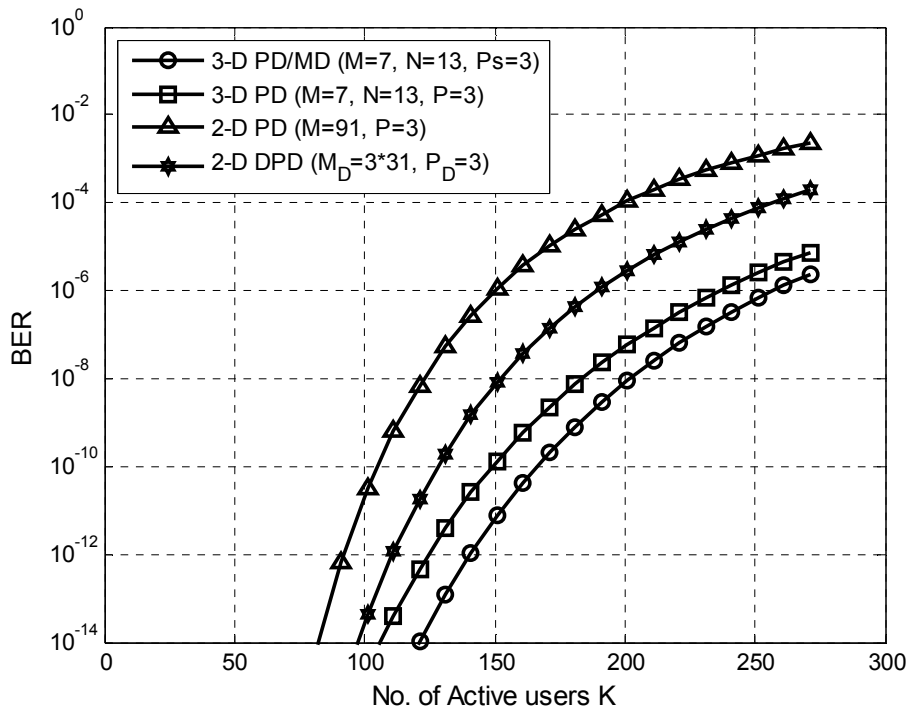


Figure 3. The BER Versus The Number Of Active Users With ($M=7, N=13, P_s=3$) Of 3-D PD/MD Code When The Effective Power $P_{sr} = -10\text{dBm}$ And Data Rate Is 0.622Gbps

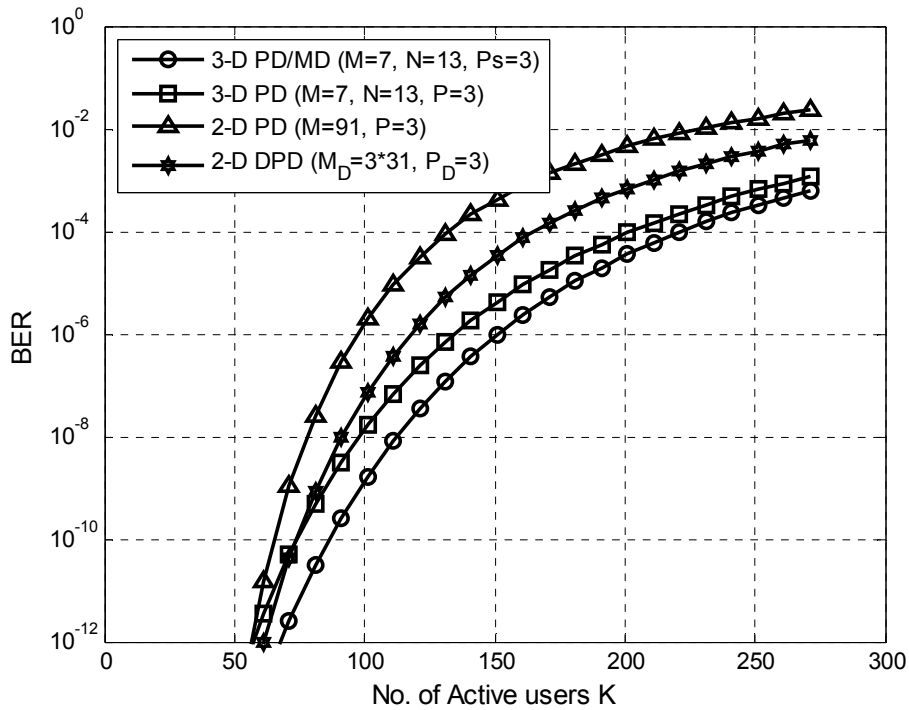


Figure 4. The BER Versus The Number Of Active Users With $(M=7, N=13, P_s=3)$ Of 3-D PD/MD Codes When The Effective Power Is $P_{sr} = -10\text{dBm}$ And Data Rate Is 1.25Gbps

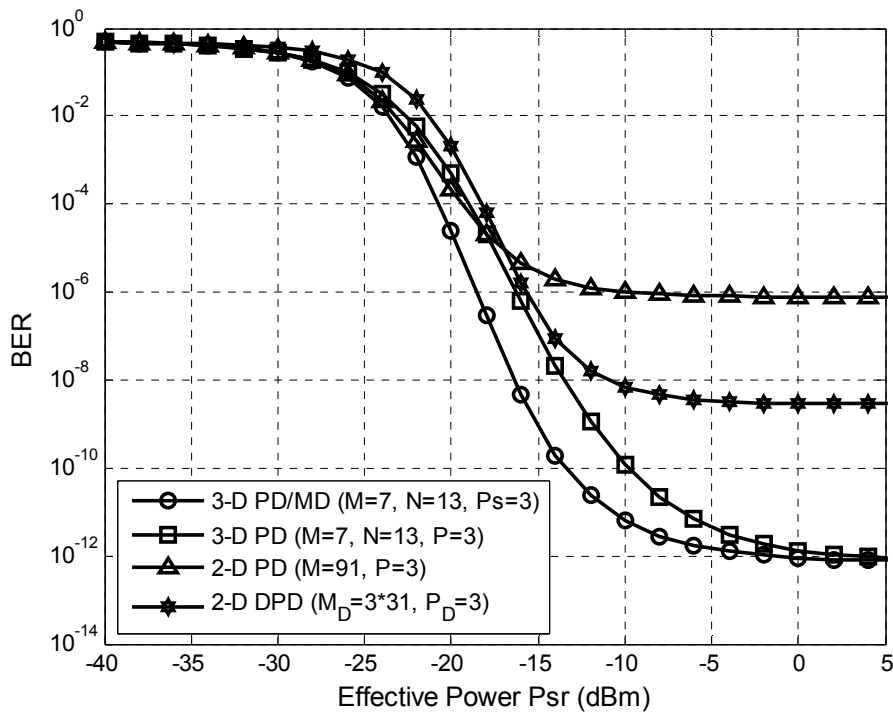


Figure 5. The BER Versus The Effective Power P_{sr} With $(M=7, N=13, P_s=3)$ Of 3-D PD/MD Code When The Number Of Active Users Is $K = 150$ And Data Rate Is 0.622Gbps.

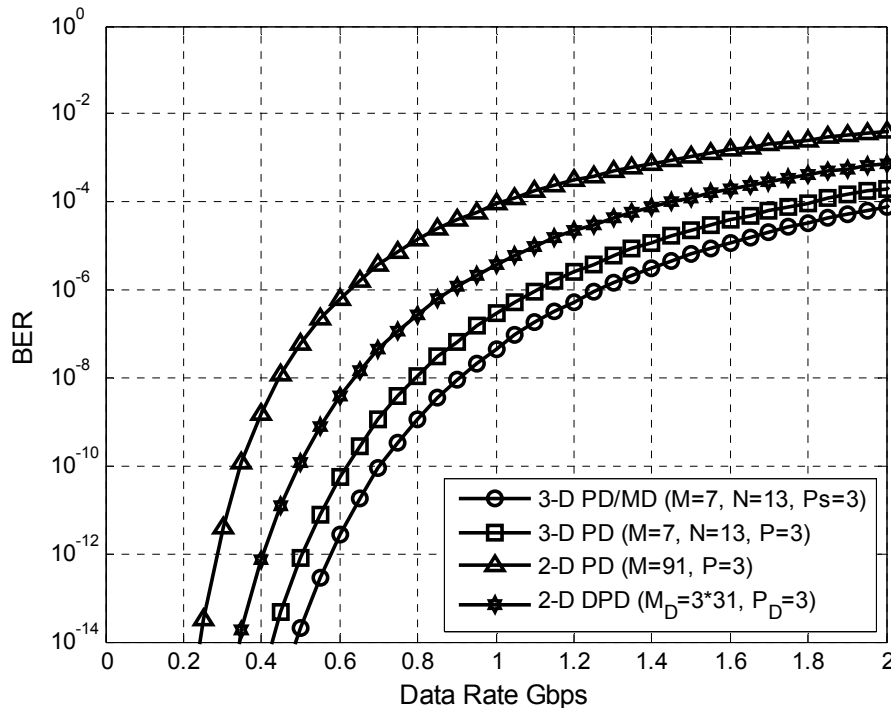


Figure 6. The BER Versus The Data Rate With ($M=7, N=13, P_s=3$) Of 3-D PD/MD Code When The Number Of Active Users Is $K=150$ And $P_{sr}=-10\text{dbm}$.

6. CONCLUSION

A new family of a three dimensional spectral/time/spatial code is presented for OCDMA systems. The generation and analysis of the code are given. In comparison to the 3-D PD code that reported previously, the proposed code reduces the receiver complexity to 50%. However, the proposed code can't accommodate much more active users than the 3-D PD code, but the reduction in the receiver complexity is the attractive feature that make it more applicable in practical systems.

REFERENCES:

- [1] F. R. K. Chung, J. Salehi, and V. K. Wei, "Optical orthogonal codes: design, analysis and applications," *Inf. Theory, IEEE Trans.*, vol. 35, no. 3, pp. 595–604, 1989.
- [2] G.-C. Yang and W. C. Kwong, "Performance analysis of optical CDMA with prime codes," *Electron. Lett.*, vol. 31, no. 7, pp. 569–570, 1995.
- [3] C. S. Weng and J. Wu, "Perfect difference codes for synchronous fiber-optic CDMA communication systems," *J. Light. Technol.*, vol. 19, no. 2, pp. 186–194, 2001.
- [4] D. Zaccarin and M. Kavehrad, "An optical CDMA system based on spectral encoding of LED," *Photonics Technol. Lett. IEEE*, vol. 5, no. 4, pp. 479–482, 1993.
- [5] M. Kavehrad and D. Zaccarin, "Optical code-division-multiplexed systems based on spectral encoding of noncoherent sources," *Light. Technol. J.*, vol. 13, no. 3, pp. 534–545, 1995.
- [6] Z. Wei, H. M. H. Shalaby, and H. Ghafouri-Shiraz, "Modified quadratic congruence codes for fiber Bragg-grating-based spectral-amplitude-coding optical CDMA systems," *Light. Technol. J.*, vol. 19, no. 9, pp. 1274–1281, 2001.
- [7] Z. Wei and H. Ghafouri-Shiraz, "Unipolar codes with ideal in-phase cross-correlation for spectral amplitude-coding optical CDMA systems," *Commun. IEEE Trans.*, vol. 50, no. 8, pp. 1209–1212, 2002.
- [8] Z. Wei and H. Ghafouri-Shiraz, "Codes for spectral-amplitude-coding optical CDMA systems," *J. Light. Technol.*, vol. 20, no. 8, p. 1284, 2002.
- [9] T. H. Abd, S. A. Aljunid, H. A. Fadhil, R. A. Ahmad, and N. M. Saad, "Development of a new code family based on SAC-



- OCDMA system with large cardinality for OCDMA network,” *Opt. Fiber Technol.*, vol. 17, no. 4, pp. 273–280, 2011.
- [10] C.-C. Yang and J.-F. Huang, “Two-dimensional M-matrices coding in spatial/frequency optical CDMA networks,” *Photonics Technol. Lett. IEEE*, vol. 15, no. 1, pp. 168–170, 2003.
- [11] C. H. Lin, J. Wu, and C. L. Yang, “Noncoherent spatial/spectral optical CDMA system with two-dimensional perfect difference codes,” *J. Light. Technol.*, vol. 23, no. 12, pp. 3966–3980, 2005.
- [12] H. Yin, L. Ma, H. Li, and L. Zhu, “A new family of 2D wavelength/time codes with large cardinality for incoherent spectral amplitude coding OCDMA networks and analysis of its performance,” *Photonic Netw. Commun.*, vol. 19, no. 2, pp. 204–211, 2009.
- [13] B.-C. Yeh, C.-H. Lin, C.-L. Yang, and J. Wu, “Noncoherent spectral/spatial optical CDMA system using 2-D diluted perfect difference codes,” *J. Light. Technol.*, vol. 27, no. 13, pp. 2420–2432, 2009.
- [14] B. Yeh, C. Lin, J. Wu, and L. Fellow, “Noncoherent Spectral / Time / Spatial Optical CDMA System Using 3-D Perfect Difference Codes,” vol. 27, no. 6, pp. 744–759, 2009.